

# Aligned SiC Porous Nanowire Arrays with Excellent Field Emission Properties Converted from Si Nanowires on Silicon Wafer

Yajun Yang,<sup>†</sup> Guowen Meng,<sup>\*,†</sup> Xianyun Liu,<sup>‡</sup> Lide Zhang,<sup>†</sup> Zheng Hu,<sup>\*,§</sup> Chengyu He,<sup>§</sup> and Yemin Hu<sup>§</sup>

Key Laboratory of Materials Physics, Anhui Key Laboratory of Nanomaterials and Nanostructures, Institute of Solid State Physics, Laboratory of Environmental Spectroscopy, Anhui Institute of Optics and Fine Mechanics, Chinese Academy of Sciences, Hefei 230031, China, and Key Laboratory of Mesoscopic Chemistry, Jiangsu Provincial Laboratory for Nanotechnology, Department of Chemistry, Nanjing University, Nanjing 210093, China

Received: October 22, 2008; Revised Manuscript Received: November 18, 2008

Highly oriented SiC porous nanowire (NW) arrays on Si substrate have been achieved via in situ carbonizing aligned Si NW arrays standing on Si substrate. The resultant SiC NW arrays inherit the diameter and length of the mother Si NW arrays. Field emission measurements show that these oriented SiC porous NW arrays are excellent field emitter with large field emission current density at very low electric field. The in situ conversion method reported here might be exploited to fabricate NW arrays of other materials containing silicon.

## 1. Introduction

Silicon carbide (SiC), a wide band gap semiconductor, has potential applications in electronic and optic devices in harsh conditions, including high temperature, high frequency, and high power,<sup>1–7</sup> owing to its low density, superplasticity, good resistance to thermal shock and oxidation, and high fracture toughness.<sup>8–14</sup> In recent years, much attention has been paid to SiC nanowires (NWs). To date, various methods have been developed to synthesize SiC NWs, including carbothermal reduction,<sup>9,12,15–17</sup> chemical vapor deposition,<sup>1,6–8,11,13,18–28</sup> chemical vapor infiltration,<sup>10,29</sup> reduction-carburization,<sup>30</sup> carbon nanotube-confined reaction,<sup>3,31,32</sup> and so forth. As  $\beta$ -SiC has an n-type wide band gap value of 2.3 eV, high electron mobility and breakdown field strength, low work function of 4.53 eV, and superior physical and chemical properties, which are prerequisites in building devices capable of generating stable emission electron current, much attention has been paid to field emission of SiC NWs.<sup>20,26,28,32–35</sup> However, SiC NWs obtained via the above-mentioned methods are randomly distributed and have disordered structures, which restrict studies on their properties and further applications. Pan et al. obtained oriented SiC NWs via carbon nanotube-confined reaction (reacting aligned carbon nanotubes with SiO).<sup>32</sup> However, the formed SiC NWs are free-standing (no substrate), it is difficult to study the field emission of these SiC NWs. Thus, it is desirable to achieve oriented SiC NW arrays on conducting substrates.

As aligned Si NW arrays could be fabricated on Si substrate through chemical-etching technique<sup>36–46</sup> and porous SiC can be

achieved by converting porous Si,<sup>47</sup> here we demonstrate the synthesis of oriented SiC porous NW arrays on Si substrate by carbonizing aligned Si NW arrays on Si substrate using ethanol as carbon element source. The resultant oriented SiC porous NW arrays on Si substrate show excellent field-emitting properties as revealed by the current–voltage characteristics.

## 2. Experimental Section

The synthesis of aligned Si NW arrays on Si wafers were conducted in a Teflon-lined stainless steel autoclave via a selective chemical-etching technique. The autoclave was filled with etching solutions containing 5.0 mol L<sup>-1</sup> HF and 0.02 mol L<sup>-1</sup> AgNO<sub>3</sub> solution. Monocrystalline n-type silicon (100) wafers (0.004  $\Omega$  cm) were initially cleaned with ethanol to remove organic grease and then immersed into the etching solutions and treated at 50 °C for 90 min. After the etching process, the Si wafers were cleaned with deionized water, and then immersed into HNO<sub>3</sub> solution to remove the Ag film deposited on the Si NW arrays. The as-prepared Si NW arrays standing on Si wafers loaded in a ceramic boat were put into the hot zone of a horizontal tubular furnace. The system was heated up to 1350 °C in 15 min and held at this temperature for 2 h. Ethanol was used as carbon source in our experiment. A constant gas flow of Ar (purity: 99.999%), serving as carrier gas, went through ethanol at a flow rate of 60 sccm (standard cubic centimeter per minute) and was maintained during both heating and cooling processes. After the reaction was terminated and the furnace was cooled to room temperature, the products were exposed to air and heated at 600 °C for about 4 h to get rid of superfluous carbon. Finally, light blue products of SiC NWs were achieved on the surface of the Si wafers. The as-synthesized products were characterized by using scanning electron microscopy (SEM, Sirion 200) and transmission electron microscopy (TEM, JEOL 2010).

\* To whom correspondence should be addressed. E-mail: gwmeng@issp.ac.cn; zhenghu@nju.edu.cn.

<sup>†</sup> Institute of Solid State Physics, Chinese Academy of Sciences.

<sup>‡</sup> Anhui Institute of Optics and Fine Mechanics, Chinese Academy of Sciences.

<sup>§</sup> Nanjing University.

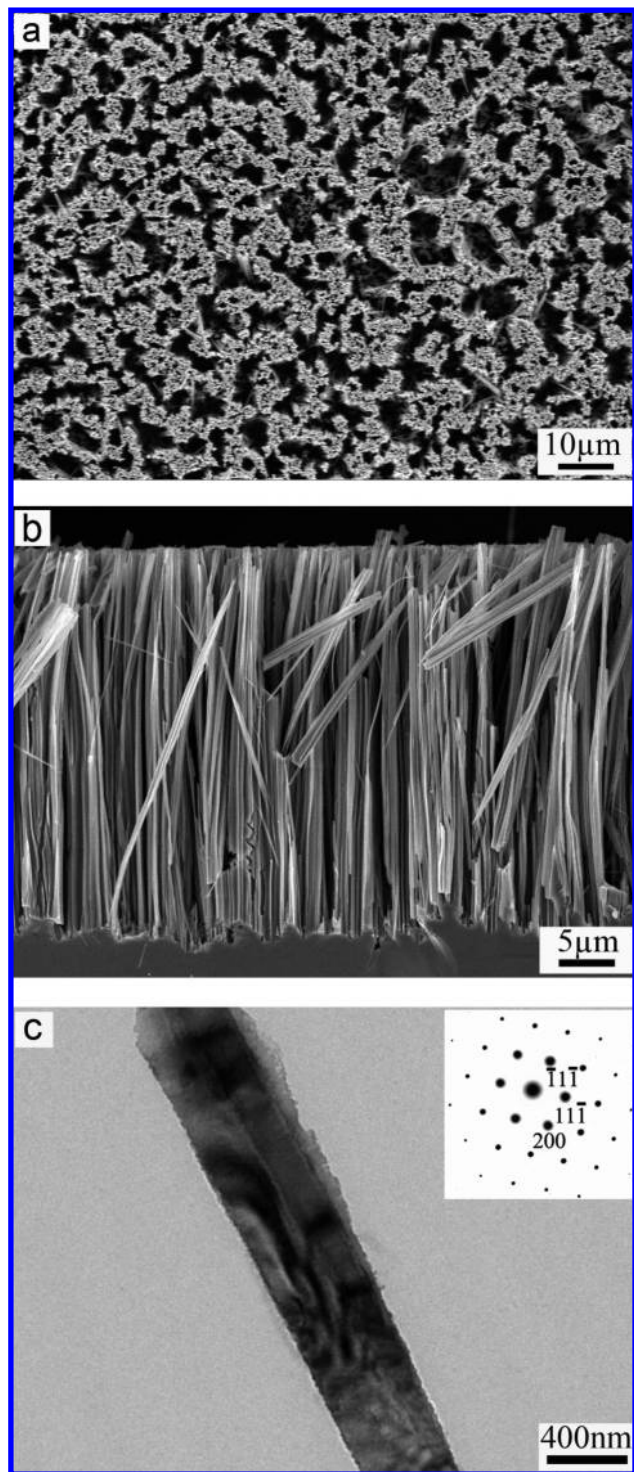


**Figure 1.** Si NW arrays: (a) top view and (b) cross-sectional view SEM images. (c) TEM image and SAED pattern (inset) of a typical Si NW.

### 3. Results and Discussion

Scanning electron microscopy (SEM) images (Figure 1a,b) reveal the oriented Si NWs bundle on the Si wafers. The individual Si NWs are about 20  $\mu\text{m}$  long with diameters from tens to hundreds of nanometers in diameter. It should be mentioned that most of the NWs have disordered microstructures with irregular cylindrical shapes. Figure 1c is a transmission electron microscopy (TEM) image of a single Si NW, revealing that Si NW is solid (rather than porous) with rough surface. Selected area electron diffraction (SAED) pattern is taken along

the  $[01\bar{1}]$  zone axis, perpendicular to this Si NW, revealing that the Si NW is single crystal. Basically, the conventional electroless metal deposition cannot control the diameter because multiple process factors are involved simultaneously in its galvanic reaction, so that the diameter of Si NWs formed has a wide distribution.<sup>44</sup> The roughness and irregular morphology of Si NW arrays may be attributed to randomness of the lateral oxidation and etching in the corrosive aqueous solution or slow HF etching and faceting of the lattice.<sup>40</sup> The growth of Si NW arrays on a silicon wafer in  $\text{AgNO}_3$  and HF solution by a selective etching of the silicon wafer is based on the principle of microelectrochemical redox reaction.<sup>36</sup> Ag deposition from HF solution is a localized microelectrochemical redox reaction process in which both anodic and cathodic processes occur simultaneously at the silicon surface.<sup>48</sup> More specifically, Ag atoms depositing on the silicon surface could form nuclei that act as a cathode, and the area surrounding these nuclei acts as an anode and will be etched away and dissolved into the solution.

Figure 2a–c shows the morphology of the converted SiC porous NW arrays through carbonization of the Si NW arrays at 1350  $^\circ\text{C}$  for 2 h using ethanol as the source of active C species. The cross-sectional views (Figure 2b,c) reveal that the converted SiC NWs have diameters ranging from tens to hundreds nanometers with lengths about 20  $\mu\text{m}$ , being similar to those of the mother Si NWs, but have much more roughness and disordered microstructures. It should be mentioned that the resultant SiC NWs are porous rather than solid, as revealed by TEM observation (Figure 2d), consisting of interconnected nanosized crystallites of SiC. The pore sizes of the SiC porous nanowires were randomly distributed from tens to hundreds of nanometers. SAED pattern (insert of Figure 2d) displays three diffraction rings assigned to the (111), (220), and (311) planes, providing further evidence that the converted SiC porous NWs have random orientation. The formation of the SiC porous NWs can be attributed to partial evaporation of Si atoms from Si NWs and carbonization of remaining Si NWs at high temperature. At the heating temperature of 1350  $^\circ\text{C}$ , some of the Si atoms are released from individually separated Si NWs on Si substrate, leading to Si porous NWs on Si substrate. In the meantime, the remaining porous Si NWs react with active carbon species decomposed from  $\text{C}_2\text{H}_5\text{OH}$  to form porous SiC. After carbonization for 2 h, the mother Si NWs were completely converted into SiC porous NWs. For simplicity, Figure 3 schematically depicts the formation process of SiC porous NW arrays.

Field emission measurements were carried out in a vacuum chamber at a pressure of  $\sim 2.0 \times 10^{-4}$  Pa at room temperature. SiC porous NW arrays standing on n-type Si wafer were used as cathode and a stainless steel plate with a diameter of 2 cm was used as anode. The cathode was connected to a 1.084 M $\Omega$  resistor. A variable positive voltage up to 5 kV was applied to the anode. The separation distance ( $d$ ) between the emitting surface and the stainless steel plate was determined by lowering the stainless steel plate to the sample until electric contact was observed and then lifting the stainless steel plate to a certain distance. The electric field ( $E$ ) was estimated via dividing the applied voltage by the anode–cathode separation distance ( $V/d$ ). The emission current density ( $J$ ) was calculated from the obtained emission current and the cathode surface area. Figure 4 shows the  $J$  of the SiC porous NW arrays as a function of the  $E$  at three anode–sample separations of 300, 400, and 500  $\mu\text{m}$ , respectively. The  $J$ – $E$  curve was obtained after sweeping the voltage several times until the electron emission was stable.



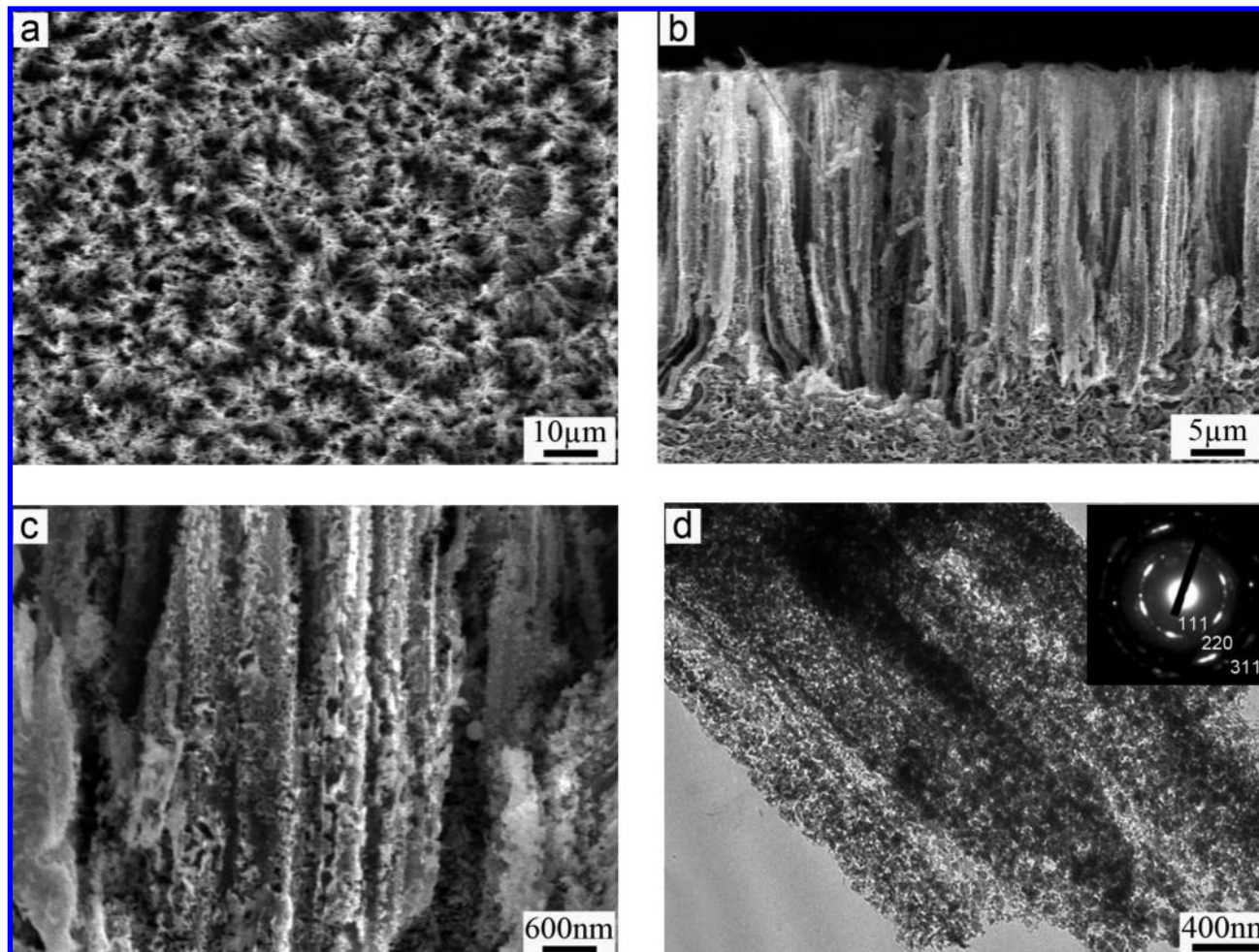


**Figure 2.** SiC porous NW arrays: (a) top view and (b,c) cross-sectional view SEM images in low- and high-magnification, respectively. (d) TEM image and SAED pattern (inset) of SiC porous NW arrays.

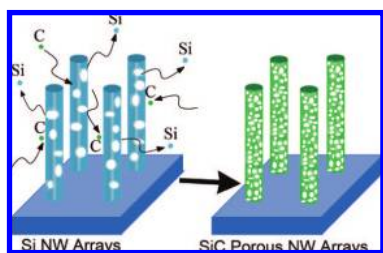


**Figure 3.** Schematic for converting Si NWs to SiC porous NWs on Si substrate.

Here, the turn-on field ( $E_{to}$ ) is defined as the field required for generating an emission current of  $10 \mu\text{A cm}^{-2}$ . It can be seen that the  $E_{to}$  depends on the  $d$  ( $E_{to}$  increases with the decrease of  $d$ ), and the  $E_{to}$  was measured to be 2.9, 2.7, and 2.3  $\text{V } \mu\text{m}^{-1}$ , respectively.

The field emission current–voltage characteristics of the SiC porous NW arrays was further analyzed on the basis of the Fowler–Nordheim (FN) theory.<sup>49</sup> That is,  $J = (A\beta^2 E^2 / \phi) \exp[-B\phi^{3/2}/E]$ , where  $J$  is the current density,  $E$  is the applied field,  $\phi$  is the work function of the emitting material,  $\beta$  is the field enhancement factor, and  $A$  and  $B$  are constants with values of  $1.54 \times 10^{-6}$  ( $\text{A eV/V cm}$ ) and  $6.83 \times 10^7$  ( $\text{V eV}^{-3/2} \text{ cm}^{-1}$ ), respectively. A typical FN plot is a plot of  $\ln(J/E^2)$  versus ( $E^{-1}$ ), which should yield a straight line for a field emission phenomenon. Figure 5 shows the corresponding FN plot of the SiC porous NW arrays at different anode-sample separations. The

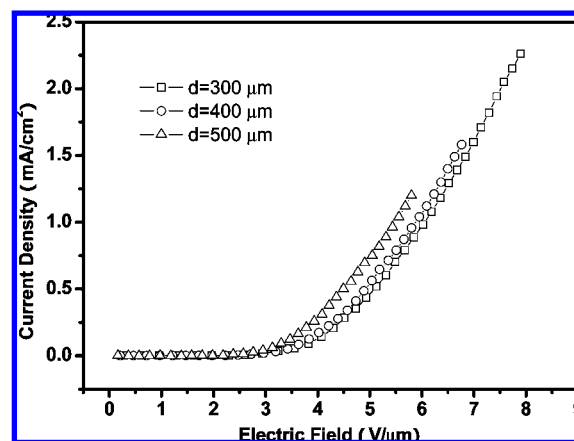


**Figure 4.** The dependence of the field-emission current density  $J$  on the applied electric field strength  $E$  of the samples at three anode-sample distances of 300, 400, and 500  $\mu\text{m}$ , respectively.

linearity of these curves shows a conventional field emission mechanism for our oriented SiC porous NW arrays. Taking the work function of SiC as 4.53 eV, the field enhancement factor  $\beta$  was calculated to be about 5241, which is much higher than those reported previously.<sup>50,51</sup>

Measurement of the emission stability was carried out on the SiC porous NW arrays at anode-sample separation of 300  $\mu\text{m}$  (Figure 6). The results show that field emission current density of  $0.57 \text{ mA cm}^{-2}$  was recorded for a period of 1200 min at the

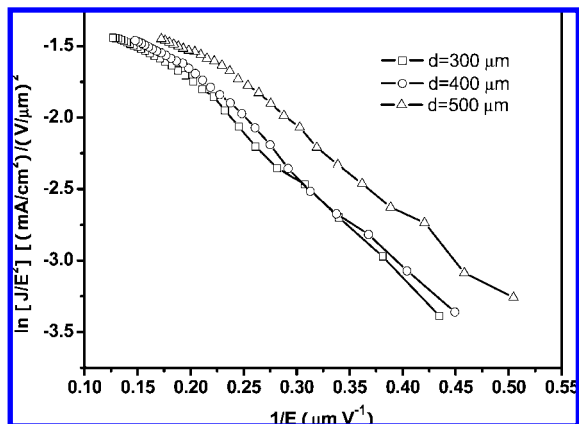


**Figure 5.** Fowler–Nordheim relationship of  $\ln(J/E^2) - 1/E$  plot at three anode-sample distances of 300, 400, and 500  $\mu\text{m}$ , respectively.

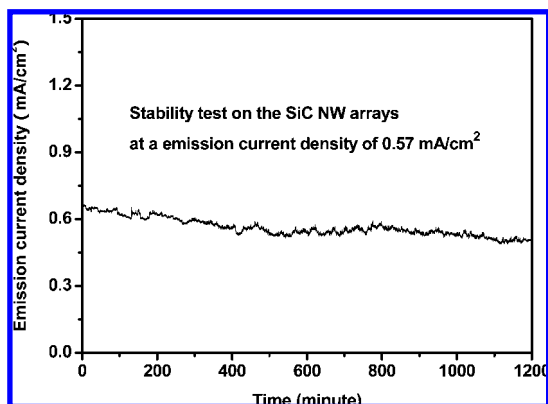


**Figure 6.** Time dependence of the emission current of SiC porous NW arrays at constant applied voltage (3000 V) and anode-sample separation (300  $\mu\text{m}$ ).

same applied voltage of 3000 V. No obvious degradation of current density was observed over this period, indicating that the aligned SiC porous NW arrays have excellent emitting behavior with potential applications in field emission technology.

#### 4. Conclusions

In summary, we have demonstrated a simple and effective method to fabricate SiC porous NW arrays by in situ conversion of Si NW arrays on Si substrate. The resultant SiC NW arrays inherit the diameter and length of the mother Si NW arrays. The SiC porous NW arrays show good field emission properties as revealed by the current–voltage characteristics. The resultant SiC NW arrays have potentials in electron field-emitting devices and might also be used as reinforcing and toughening elements in ceramic, metal, and polymer matrix composites. The method reported here might be exploited to fabricate NWs arrays of other materials containing silicon.

**Acknowledgment.** This work was financially supported by the National Science Fund for Distinguished Young Scholars (Grant 50525207), the National Basic Research Program of China (Grant 2007CB936601), “973” programs (2007CB936302), NSFC (20525312, 20471028), and MOE (NCET-04-0449, 20040284006).

#### References and Notes

- (1) Li, Y. B.; Dorozhkin, P. S.; Bando, Y.; Golberg, D. *Adv. Mater.* **2005**, *17*, 545.
- (2) Papanikolaou, N. *J. Phys.: Condens. Matter* **2008**, *20*, 135201.

- (3) Sun, X. H.; Li, C. P.; Wong, W. K.; Wong, N. B.; Lee, C. S.; Lee, S. T.; Teo, B. K. *J. Am. Chem. Soc.* **2002**, *124*, 14464.
- (4) Yang, G. Y.; Wu, R. B.; Chen, J. J.; Pan, Y.; Zhai, R.; Wu, L. L.; Lin, J. *Nanotechnology* **2007**, *18*, 155601.
- (5) Saulig-Wenger, K.; Cornu, D.; Chassagneux, F.; Ferro, G.; Epicier, T.; Miele, P. *Solid State Commun.* **2002**, *124*, 157.
- (6) Li, J. C.; Lee, C. S.; Lee, S. T. *Chem. Phys. Lett.* **2002**, *355*, 147.
- (7) Feng, D. H.; Jia, T. Q.; Li, X.; Xu, Z. Z.; Chen, J.; Deng, S. Z.; Wu, Z. S.; Xu, N. S. *Solid State Commun.* **2003**, *128*, 295.
- (8) Yang, Y. J.; Meng, G. W.; Liu, X. Y.; Zhu, X. G.; Kong, M. G.; Han, F. M.; Zhao, X. L.; Xu, Q. L.; Zhang, L. D. *Cryst. Growth Des.* **2008**, *8*, 1818.
- (9) Zhang, Y. F.; Han, X. D.; Zheng, K.; Zhang, Z.; Zhang, X. N.; Fu, J. Y.; Ji, Y.; Hao, Y. J.; Guo, X. Y.; Wang, Z. L. *Adv. Funct. Mater.* **2007**, *17*, 3435.
- (10) Yang, W.; Araki, H.; Hu, Q. L.; Ishikawa, N.; Suzuki, H.; Noda, T. *J. Cryst. Growth* **2004**, *264*, 278.
- (11) Li, Z. J.; Zhang, J. L.; Meng, A.; Guo, J. Z. *J. Phys. Chem. B* **2006**, *110*, 22382.
- (12) Li, J. Y.; Zhang, Y. F.; Zhong, X. H.; Yang, K. Y.; Meng, J.; Cao, X. Q. *Nanotechnology* **2007**, *18*, 245606.
- (13) Li, F.; Wen, G. J. *Mater. Sci.* **2007**, *42*, 4125.
- (14) Durandurdu, M. *Phys. Status Solidi B* **2006**, *243*, R37.
- (15) Meng, G. W.; Zhang, L. D.; Mo, C. M.; Zhang, S. Y.; Qin, Y.; Feng, S. P.; Li, H. J. *J. Mater. Res.* **1998**, *13*, 2533.
- (16) Li, K. Z.; Wei, J.; Li, H. J.; Li, Z. J.; Hou, D. S.; Zhang, Y. L. *Mater. Sci. Eng., A* **2007**, *460*, 233.
- (17) Wang, W.; Jin, Z.; Xue, T.; Yang, G.; Qiao, G. *J. Mater. Sci.* **2007**, *42*, 6439.
- (18) Guo, J. Z.; Zuo, Y.; Li, Z. J.; Gao, W. D.; Zhang, J. L. *Phys. E* **2007**, *39*, 262.
- (19) Kim, W. J.; Kang, S. M.; Jung, C. H.; Park, J. Y.; Ryu, W. S. *J. Cryst. Growth* **2007**, *300*, 503.
- (20) Zhou, W. M.; Wu, Y. J.; Kong, E. S. W.; Zhu, F.; Hou, Z. Y.; Zhang, Y. F. *Appl. Surf. Sci.* **2006**, *253*, 2056.
- (21) Meng, G. W.; Zhang, L. D.; Qin, Y.; Philipp, F.; Qiao, S. R.; Guo, H. M.; Zhang, S. Y. *Chin. Phys. Lett.* **1998**, *15*, 689.
- (22) Baek, Y.; Ryu, Y.; Yong, K. *Mater. Sci. Eng., C* **2006**, *26*, 805.
- (23) Frechette, J.; Carraro, C. *J. Am. Chem. Soc.* **2006**, *128*, 14774.
- (24) Meng, A.; Li, Z. J.; Zhang, J. L.; Gao, L.; Li, H. J. *J. Cryst. Growth* **2007**, *308*, 263.
- (25) Yao, X. M.; Tan, S. H.; Huang, Z. R.; Dong, S. M.; Jiang, D. L. *Ceram. Int.* **2007**, *33*, 901.
- (26) Tang, C. C.; Bando, Y. *Appl. Phys. Lett.* **2003**, *83*, 659.
- (27) Zhu, Y. Q.; Hu, W. B.; Hsu, W. K.; Terrones, M.; Grobert, N.; Hare, J. P.; Kroto, H. W.; Walton, D. R. M.; Terrones, H. *J. Mater. Chem.* **1999**, *9*, 3173.
- (28) Shen, G. Z.; Bando, Y.; Ye, C. H.; Liu, B. D.; Golberg, D. *Nanotechnology* **2006**, *17*, 3468.
- (29) Yang, W.; Araki, H.; Tang, C. C.; Thaveethavorn, S.; Kohyama, A.; Suzuki, H.; Noda, T. *Adv. Mater.* **2005**, *17*, 1519.
- (30) Hu, J. Q.; Lu, Q. K.; Tang, K. B.; Deng, B.; Jiang, R. R.; Qian, Y. T.; Yu, W. C.; Zhou, G. E.; Liu, X. M.; Wu, J. X. *J. Phys. Chem. B* **2000**, *104*, 5251.
- (31) Wu, R. B.; Pan, Y.; Yang, G. Y.; Gao, M. X.; Wu, L. L.; Chen, J. J.; Zhai, R.; Lin, J. *J. Phys. Chem. C* **2007**, *111*, 6233.
- (32) Pan, Z. W.; Lai, H. L.; Au, F. C. K.; Duan, X. F.; Zhou, W. Y.; Shi, W. S.; Wang, N.; Lee, C. S.; Wong, N. B.; Lee, S. T.; Xie, S. S. *Adv. Mater.* **2000**, *12*, 1186.
- (33) Wong, K. W.; Zhou, X. T.; Au, F. C. K.; Lai, H. L.; Lee, C. S.; Lee, S. T. *Appl. Phys. Lett.* **1999**, *75*, 2918.
- (34) Ryu, Y.; Park, B.; Song, Y.; Yong, K. J. *J. Cryst. Growth* **2004**, *271*, 99.
- (35) Deng, S. Z.; Li, Z. B.; Wang, W. L.; Xu, N. S.; Zhou, J.; Zheng, X. G.; Xu, H. T.; Chen, J.; She, J. C. *Appl. Phys. Lett.* **2006**, *89*, 023118.
- (36) Peng, K. Q.; Yan, Y. J.; Gao, S. P.; Zhu, J. *Adv. Mater.* **2002**, *14*, 1164.
- (37) Peng, K. Q.; Huang, Z. P.; Zhu, J. *Adv. Mater.* **2004**, *16*, 73.
- (38) Garnett, E. C.; Yang, P. D. *J. Am. Chem. Soc.* **2008**, *130*, 9224.
- (39) Peng, K. Q.; Xu, Y.; Wu, Y.; Yan, Y. J.; Lee, S. T.; Zhu, J. *Small* **2005**, *1*, 1062.
- (40) Hochbaum, A. I.; Chen, R. K.; Delgado, R. D.; Liang, W. J.; Garnett, E. C.; Najarian, M.; Majumdar, A.; Yang, P. D. *Nature* **2008**, *451*, 163.
- (41) Peng, K. Q.; Wang, X.; Lee, S.-T. *Appl. Phys. Lett.* **2008**, *92*, 163103.
- (42) Huang, Z. P.; Zhang, X. X.; Reiche, M.; Liu, L. F.; Lee, W.; Shimizu, T.; Senz, S.; Gösele, U. *Nano Lett.* **2008**, *8*, 3046.
- (43) Peng, K. Q.; Yan, Y. J.; Gao, S. P.; Zhu, J. *Adv. Funct. Mater.* **2003**, *13*, 127.

- (44) Chen, C.-C.; Wu, C.-S.; Chou, C.-J.; Yen, T.-J. *Adv. Mater.* **2008**, *20*, 3811.
- (45) Peng, K. Q.; Wu, Y.; Fang, H.; Zhong, X. Y.; Xu, Y.; Zhu, J. *Angew. Chem., Int. Ed.* **2005**, *44*, 2737.
- (46) Cheng, S. L.; Chung, C. H.; Lee, H. C. *J. Electrochem. Soc.* **2008**, *155*, D711.
- (47) Yang, Y. J.; Meng, G. W.; Liu, X. Y.; Zhang, L. D. *Angew. Chem., Int. Ed.* **2008**, *47*, 365.
- (48) Gorostiza, P.; Kulandainathan, M. A.; Diaz, R.; Sanz, F.; Allongue, P.; Morante, J. R. *J. Electrochem. Soc.* **2000**, *147*, 1026.

- (49) Fowler, R. H.; Nordheim, L. *Proc. R. Soc. London, Ser. A* **1928**, *119*, 173.
- (50) Kim, D.-W.; Choi, Y.-J.; Choi, K. J.; Park, J.-G.; Park, J.-H.; Pimenov, S. M.; Frolov, V. D.; Abanshin, N. P.; Gorfinkel, B. I.; Rossukanyi, N. M.; Rukovichnikov, A. I. *Nanotechnology* **2008**, *19*, 225706.
- (51) Wu, Z. S.; Deng, S. Z.; Xu, N. S.; Chen, J.; Zhou, J.; Chen, J. *Appl. Phys. Lett.* **2002**, *80*, 3829.

JP809359V